ChemComm
Chemical Communications

## Accepted Manuscript

This article can be cited before page numbers have been issued, to do this please use: H. T. H. Nguyen and L. Do, *Chem. Commun.*, 2020, DOI: 10.1039/D0CC04970K.




ROYAL SOCIETY OF CHEMISTRY

rsc.li/chemcomm

View Article Online
DOI: 10.1039/D0CC04970K

COMMUNICATION

# Organoiridium-Quinone Conjugates for Facile Hydrogen Peroxide Generation

Received 00th January 20xx,
Accepted 00th January 20xx

DOI: 10.1039/x0xx00000x

Huong T. H. Nguyen, Loi H. Do*



**An organoiridium complex bearing a quinone moiety was shown to significantly accelerate the rate of $H_2O_2$ formation in the presence of air and sodium formate at low catalyst concentrations. This reaction is proposed to operate through a synergistic mechanism involving transfer hydrogenation catalysis and radical chemistry. Our bifunctional iridium complex could potentially be used in anti-cancer chemotherapy or other applications requiring rapid generation of reactive oxygen species.**

Reactive oxygen species (ROS), such as peroxide, superoxide, and hydroxyl radical, play critical roles in essential biochemical functions as well as pathological processes.[1] Strategies exploiting ROS to selectively kill cancer cells have shown clinical promise.[2] They include the use of agents to increase endogenous ROS, inhibit natural antioxidant enzymes, or deplete glutathione concentrations. Although synthetic compounds that induce ROS can operate by distinct mechanisms, achieving high efficiency and selectivity are still major challenges. A recent advance in ROS generating agents is the discovery by Sadler and co-workers that half-sandwich organoiridium complexes could catalyse the formation of hydrogen peroxide from $O_2$, $H^+$, and reduced nicotinamide adenine dinucleotide (NADH) via a transfer hydrogenation mechanism (Scheme 1).[3] These Ir compounds were demonstrated to have more potent anti-cancer activity than the well-known drug cisplatin in some cell lines. Later in 2016, Suenobu, Fukuzumi, and co-worker showed that 2,3-dimethoxy-6-methyl-1,4-benzoquinone (**Q1**) and organoiridium compounds react with NADH and $O_2$ to produce $H_2O_2$ in a tandem catalytic process.[4]

The iridium/**Q1** example above is particularly intriguing because the coupling of transfer hydrogenation with autocatalytic $O_2$ reduction could significantly boost $H_2O_2$ formation.[4] However, a possible concern with this dual component system is that at low catalyst concentrations (e.g., <50 μM), which is typically recommended for cell studies to minimize possible metal toxicity, the iridium and **Q1** species have a low probability of reacting with one another because they could be distributed to different cellular locations. To circumvent this potential problem, we propose that the organoiridium complex be covalently tethered to a quinone group to promote *intramolecular* reactivity. The benefits of this bifunctional catalyst design are that both iridium-hydride and hydroquinone units formed during reactions with NADH are capable of reducing $O_2$ to $H_2O_2$ and oxidized quinone could be continuously regenerated regardless of catalyst concentration. This strategy of incorporating redox active moieties into transition metal complexes has been shown to be highly effective for a variety of catalytic applications.[5,6]

**Scheme 1**. Hydrogen peroxide formation achieved by transfer hydrogenation catalysis.

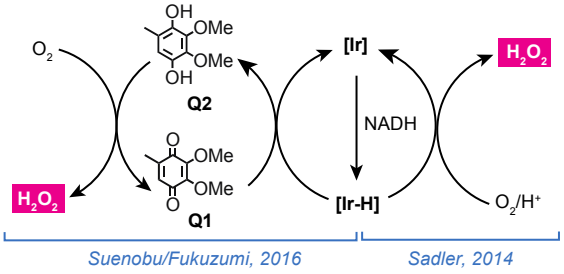


To test the feasibility of our bifunctional catalyst concept, we devised a novel molecular construct by attaching the ubiquinone mimic **Q1** to [Cp*Ir(*N*-phenylpyridinecarboxamidate)Cl] (**Ir1**, Cp* = pentamethylcyclopentadienyl anion). Complex **Ir1** was found in our previous work to be an active transfer hydrogenation catalyst under biologically relevant conditions[7,8] and inside cells.[9] The **Q1** group was tethered to **Ir1** using either an ether or alkyl linker to give complexes **Ir2** and **Ir3a**, respectively (Chart 1). The detailed syntheses of these iridium-quinone conjugates are provided in the Electronic Supplementary Information (Schemes S1-S2). The final iridium complexes were obtained in analytically pure form and characterized by various spectroscopic and mass spectrometric methods. Single

*Department of Chemistry, University of Houston, 4800 Calhoun Road, Houston, TX 77204*

Electronic Supplementary Information (ESI) available: synthesis and characterization, procedures, spectral data. See DOI: 10.1039/x0xx00000x

crystals of **Ir3a** were grown from acetone/pentane and analysed by X-ray diffraction. The molecular structure of **Ir3a** showed the expected piano-stool motif, in which the iridium centre was coordinated by a Cp* ring, two nitrogen donors from ligand **8**, and a chloride (Figure S38).

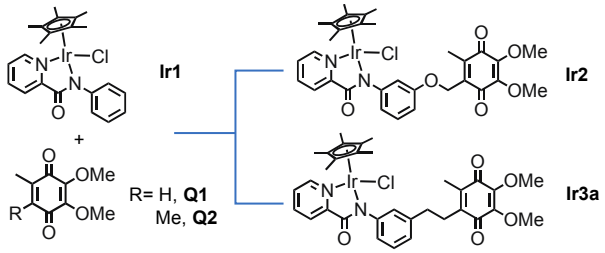


**Chart 1**. Design of organoiridium-quinone conjugates.

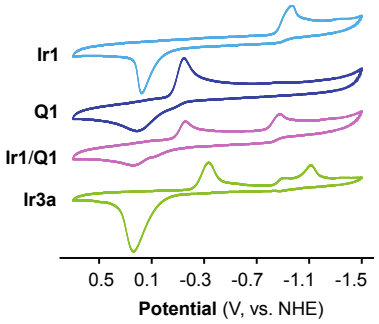


**Figure 1**. Cyclic voltammograms of iridium complexes (1.0 mM) and quinone (0.5 mM) recorded at 0.1 V/s in 0.1 M phosphate buffer saline (PBS). All potentials are referenced to NHE.

The redox behaviour of the iridium complexes was measured in phosphate buffered saline (PBS) by cyclic voltammetry (Figure 1 and S1). Complex **Ir1** displayed an irreversible reduction wave at -0.96 V and oxidation waves at -0.88 (weak) and 0.19 V vs. NHE, similar to those reported in our previous work.[8] Compound **Q1** exhibited a reduction peak at -0.13 V and oxidation peak at 0.22 V. The combined **Ir1** and **Q1** (1:1) sample showed cathodic processes occurring at -0.86 and -0.15 V. Surprisingly, the former peak shifted from that of **Ir1** by about +0.10 V. Studies by $^1$H NMR spectroscopy suggest that this shift in reduction potential is *not* due to coordination interaction between **Q1** with the iridium complex (Figure S12). Even upon chloride abstraction by treating **Ir1** with AgOTf in $CD_3OD/D_2O$ (4:1),[8] the resulting iridium-solvato species does not appear to bind quinone. We hypothesize that perhaps weak outer sphere interactions (e.g., halogen bonding[10]) between **Ir1** and **Q1** might be responsible for the Ir-centered redox potential change.

The CV of **Ir3a** displayed reduction peaks at -1.10, -0.89, and -0.32 V and oxidation peaks at -0.87 (weak) and 0.25 V (Figure 1 and S1). The cathodic process at -0.32 V was attributed to reduction of the quinone ring. This potential is similar to that observed in the CV of **Q2** ($E_{red}$= -0.26 V, Figure S2), which is expected given that **Q2** has a 5-methyl group analogous to the alkyl chain attached to the quinone ring in **Ir3a**. We presume that the peaks at -1.10 and -0.89 V correspond to iridium-based reductions but are uncertain why there are two peaks in this region since **Ir1** showed only one. One possibility is that **Ir3a** coordinates to each other intermolecularly to give a mixture of monometallic and multimetallic species. However, further studies are needed to determine the nuclearity of **Ir3a** in solution.

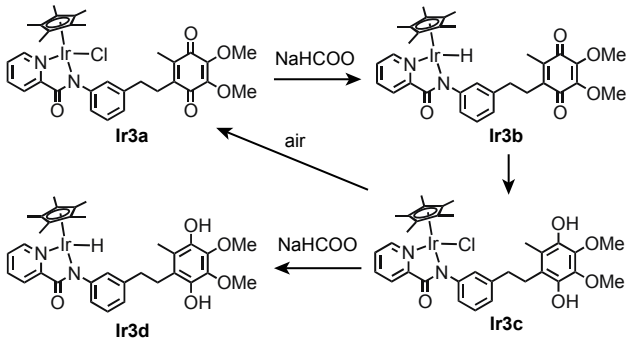


**Scheme 2**. Reaction of **Ir3a** with NaHCOO in $CD_3OD$ studied by variable temperature NMR spectroscopy.

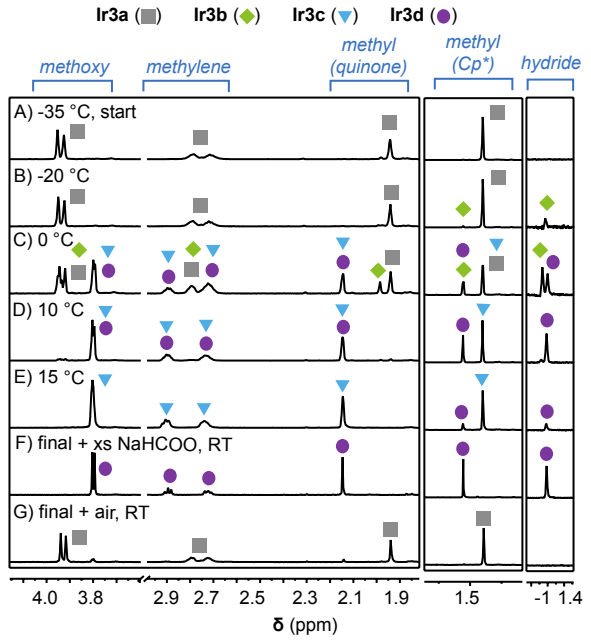


**Figure 2**. $^1$H NMR spectra ($CD_3OD$, 600 MHz) of the reaction of **Ir3a** (5 mM) with NaHCOO (10 mM) studied at variable temperature. The reactants were mixed at -35 °C (part A) and then allowed to warm up to -20 (B), 0 (C), 10 (D), and 15 (E) °C. The final sample was either treated with excess NaHCOO (F) or exposed to air (G) overnight.

To establish whether our iridium-quinone conjugates are competent transfer hydrogenation catalysts, we first evaluated their reactions with sodium formate. Because both NADH and NaHCOO hydride sources are compatible with organoiridium complexes,[7] we used the latter because it does not have $^1$H NMR peaks that overlap in the spectral regions of interest. When a 5 mM solution of **Ir2** in acetone-$d_6$ was combined with 5.0 equiv. of NaHCOO *in air*, complete catalyst decomposition was observed within 16 h, most likely due to oxidative cleavage of its benzyl ether bond by the hydrogen peroxide generated (Figure S9). In contrast, no catalyst decomposition occurred using **Ir3a** under similar reaction conditions.

Because of its greater chemical stability, **Ir3a** was subjected to more detailed reaction studies. At RT, reaction of **Ir3a** with

View Article Online
DOI: 10.1039/D0CC04970K

excess NaHCOO led to quantitative conversion to the reduced hydroquinone product within ~5 min (Scheme 2). To follow the reaction *in situ*, variable temperature NMR spectroscopic measurements were performed (Figure 2). When **Ir3a** and NaHCOO (1:2) were combined at -35 °C under nitrogen, only peaks corresponding to the starting iridium complex and NaHCOO were present, suggesting no reaction had taken place. Upon warming to -20 °C, a distinct signal at -11.29 ppm appeared, which is characteristic of an iridium-hydride species.[7,8] This intermediate is proposed to be the iridium-hydride/quinone complex **Ir3b** formed from decarboxylation of NaHCOO by the Ir centre. When the reaction mixture was increased to 0 °C, the formation of two additional species was apparent. Their identities were determined to be the iridium-chloride/hydroquinone (**Ir3c**) and iridium-hydride/hydroquinone (**Ir3d**) species based on comparison with the NMR spectra obtained from independently prepared samples (see ESI). Complex **Ir3c** can be formed spontaneously from **Ir3b** as a result of either intermolecular or intramolecular hydride transfer between Ir–H and quinone functionalities.[11,12] Subsequent conversion to **Ir3d** could then proceed by reaction of **Ir3c** with another equivalence of formate. Surprisingly, when the NMR sample was warmed from 10 to 15 °C, the amount of **Ir3d** decreased whereas the amount of **Ir3c** increased (*cf.* spectrum D vs. E in Figure 2). However, to establish that **Ir3d** is the most reduced product, addition of excess NaHCOO to the 15 °C sample gave quantitative amounts of **Ir3d** (spectrum F). We found that ~4 equiv. of NaHCOO is required for complete conversation of **Ir3a** to **Ir3d** (Figure S11). Since this reaction should only need two reducing equivalents rather than four, these results suggest that perhaps the Ir-H units could decay via reaction with solvent or other proton sources to produce $H_2$.[13,14] Finally, when the 15 °C sample was exposed to air overnight, the starting **Ir3a** complex was regenerated (spectrum G, Figure 2).

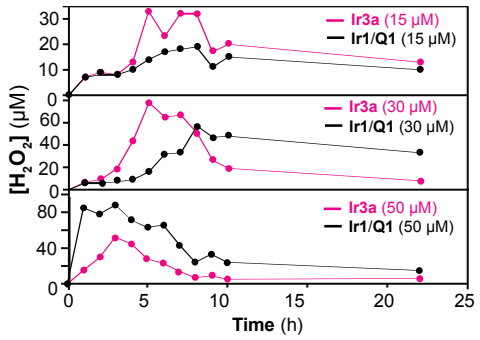


**Figure 3**. Formation of hydrogen peroxide from reaction of either **Ir3a** or **Ir1/Q1** in $H_2O$/DMSO (99:1) with 20 equiv. of NaHCOO at various catalyst concentrations. The data shown are representative plots. The absolute $H_2O_2$ concentrations can vary between repeat experiments due to limitations of the image-based $H_2O_2$ quantification method but the relative trends are consistent.

Next, the hydrogen peroxide formation efficiency was compared between the tethered vs. untethered iridium-quinone catalysts. Although a variety of $H_2O_2$ quantification methods have been reported, some used reagents that are not readily available,[15,16] incompatible with hydroquinone,[17,18] or have insufficient detection range.[19] We found that commercial $H_2O_2$ test strips provided fast response time and adequate sensitivity for our studies.[3] Using this semi-quantitative detection method combined with ImageJ software analysis, we measured the hydrogen peroxide concentration from reactions of either **Ir3a** or **Ir1/Q1** (1:1) with 20 equiv. of NaHCOO in $H_2O$/DMSO (99:1) under air (Figure S4 and S5). At lower catalyst concentrations (Figure 3, top/middle), **Ir3a** gave more hydrogen peroxide and at a faster rate than **Ir1/Q1.** For example, after 5 h, **Ir3a** produced 2.4-fold (33 vs. 14 μM) and 4.9-fold (78 vs. 16 μM) more $H_2O_2$ than **Ir1/Q1** at catalyst concentrations of 15 and 30 μM, respectively. Similar results were obtained when comparing the $H_2O_2$ forming ability of **Ir3a** vs. **Ir1/Q2** (Figure S6) at 30 μM catalyst concentration, suggesting that slight differences in the quinone redox potential do not account for the faster rate observed in the former. Interestingly, when the amount of catalyst was increased to 50 μM, the opposite trend was observed (Figure 3, bottom). After 1 h, **Ir1/Q1** gave a 5.7-fold increase in $H_2O_2$ compared to that by **Ir3a** (85 vs. 15 μM, respectively). Reaction of **Ir1** with NaHCOO provided less $H_2O_2$ than that using either **Ir3a** or **Ir1/Q1** (Figure S5), indicating that the presence of quinone had a beneficial effect. As a control, combining **Q1** with NaHCOO in the absence of iridium gave no $H_2O_2$.

The catalytic efficiency of **Ir3a** was determined by measuring its turnover number (TON). Because quantifying the total amount of $H_2O_2$ produced was problematic due to its subsequent reactivity with Ir (vide infra), changes in NaHCOO concentration was monitored instead. We observed that reaction of NaHCOO (20 μmol) with **Ir3a** (0.5 μmol) was complete after 21 h (Figure S14) and gave a TON = 40, which suggests that our iridium-quinone complex is indeed catalytic.

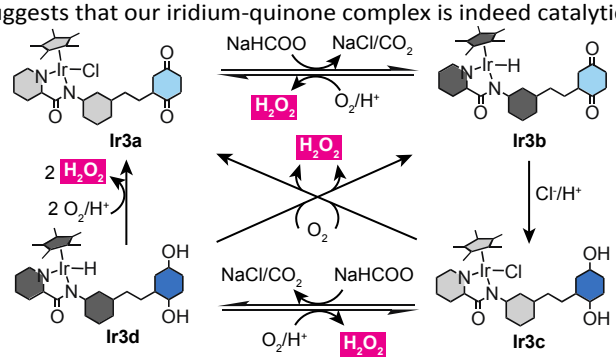


**Scheme 3**. Possible intramolecular pathways to produce $H_2O_2$ from the reaction of **Ir3a** with NaHCOO. Intermolecular reactions are also possible but less likely at low catalyst concentrations. Reaction of hydroquinone with $O_2$ could generate hydrogen peroxide autocatalytically. Structures drawn in simplified form.

The plots in Figure 3 revealed that $H_2O_2$ growth was accompanied by subsequent decay, which suggests that the hydrogen peroxide produced may be reacting with one of the reaction components. We observed that when excess $H_2O_2$ was mixed with 30 μM of **Ir1** or **Ir3a**, the hydrogen peroxide concentration gradually decreased over time. In contrast, control solutions containing $H_2O_2$ only or **Q1**/$H_2O_2$ showed no significant change in hydrogen peroxide levels over 22 h. Characterization of the $H_2O_2$-treated iridium complexes by both NMR (Figure S13) and UV-vis absorption spectroscopy showed significant catalyst decomposition, suggesting that **Ir1**

and **Ir3a** are susceptible to oxidative damage in the presence of excess hydrogen peroxide over an extended period. Attempts to determine the identity of the decomposed Ir species were unsuccessful.

To confirm that $H_2O_2$ is responsible for catalyst decay, we monitored the reaction of **Ir3a** with NaHCOO in the presence of propyl sulfide as an antioxidant (Figure S15). After 18 h, our NMR spectra showed that the sample containing $n$Pr$_2$S still contained significant amounts of **Ir3a** whereas the sample without $n$Pr$_2$S had nearly no detectable amounts of **Ir3a** present. We verified that $n$Pr$_2$S did not inhibit the Ir catalyst activity so its role was primarily an $H_2O_2$ scavenger.

We propose that the iridium-quinone and NaHCOO reactions operate by several competing pathways. In our tethered **Ir3a** catalyst, $H_2O_2$ could form from reaction of $O_2$ with **Ir3b**, **Ir3c** or **Ir3d** (Scheme 3). Because the iridium and quinone units are covalently linked, the rate of intramolecular hydride transfer to reactivate the quinone unit (i.e., **Ir3b** → **Ir3c**) is independent of catalyst concentration. Intermolecular reactions between the **Ir3a**-**Ir3d** species are also possible but less likely to occur at lower catalyst concentrations. In the untethered **Ir1**/**Q1** system, similar reaction pathways are potentially accessible. However, the key difference is that hydride transfer from **Ir1**-hydride to **Q1** is a bimolecular reaction and thus, this step is concentration dependent.[11,12] At high catalyst concentrations, we propose that the above transfer hydrogenation process to generate $H_2O_2$ is less important than the autocatalytic reaction between hydroquinone and $O_2$. In fact, studies by Suenobu/Fukuzumi and co-workers showed the rate of $H_2O_2$ formation was dependent only on the concentrations of **Q1** and $O_2$ and not iridium or NADH (when [**Q1**] > [Ir]).[4] They established that reaction of hydroquinone and $O_2$ followed a sigmoidal curve, which is indicative of autocatalysis. Our observation that **Ir3a** is more efficient at low concentration whereas **Ir1**/**Q1** is more efficient at high concentration is consistent with a switch in major vs. minor reaction pathways. More detailed kinetic studies, however, are needed to interrogate this hypothesis.

In summary, we showed for the first time that organoiridium-quinone conjugates are more efficient $H_2O_2$-generating catalysts than iridium and quinone tandem catalysts at low concentrations (<50 μM). We expect that inside living cells, the hydrogen peroxide produced by **Ir3a** would likely be scavenged by reactive biomolecules such as glutathione before having the opportunity to degrade the catalyst as observed in the reaction flask. Although we were able to achieve up to ~4.9-fold increase in $H_2O_2$ formation using **Ir3a**, we anticipate that further optimization of the iridium-quinone construct could lead to even greater rate enhancements. Our results could have important biological relevance because these studies were performed under ambient[3] rather than oxygen-enriched environments.[20] Because some of the most potent quinone-based anti-cancer agents have 50% growth inhibition concentrations below 50 μM,[21,22] they are not typically used in amounts that would allow them to fully exploit their autocatalytic $H_2O_2$ forming capabilities. Thus, our strategy of combining half-sandwich iridium complexes[23] with quinones could take advantage of synergistic reactivity to maximize their therapeutic benefits even in low-doses.

This work was supported by the Welch Foundation (Grant No. E-1894) and NIH (Grant No. R01GM129276).

## Conflicts of interest

There are no conflicts to declare.

## Notes and references

(1) Nidhi, K.; Julia, C.; Ryan, J. M. *Biol. Chem.* **2017**, *398*, 1209-1227.
(2) Trachootham, D.; Alexandre, J.; Huang, P. *Nat. Rev. Drug Discov.* **2009**, *8*, 579-591.
(3) Liu, Z.; Romero-Canelón, I.; Qamar, B.; Hearn, J. M.; Habtemariam, A.; Barry, N. P.; Pizarro, A. M.; Clarkson, G. J.; Sadler, P. J. *Angew. Chem. Int. Ed.* **2014**, *53*, 3941-3946.
(4) Suenobu, T.; Shibata, S.; Fukuzumi, S. *Inorg. Chem.* **2016**, *55*, 7747-7754.
(5) Kajetanowicz, A.; Milewski, M.; Rogińska, J.; Gajda, R.; Woźniak, K. *Eur. J. Org. Chem.* **2017**, 626-638.
(6) Kubanik, M.; Lam, N. Y. S.; Holtkamp, H. U.; Söhnel, T.; Anderson, R. F.; Jamieson, S. M. F.; Hartinger, C. G. *Chem. Commun.* **2018**, *54*, 992-995.
(7) Ngo, A. H.; Ibañez, M.; Do, L. H. *ACS Catal.* **2016**, *6*, 2637-2641.
(8) Ngo, A. H.; Do, L. H. *Inorg. Chem. Front.* **2020**, *7*, 583-591.
(9) Bose, S.; Ngo, A. H.; Do, L. H. *J. Am. Chem. Soc.* **2017**, *139*, 8792-8795.
(10) Mandal, K.; Bansal, D.; Kumar, Y.; Rustam; Shukla, J.; Mukhopadhyay, P. *Chem. Eur. J.* **2020**, *26*, 10607-10619.
(11) Liu, Z.; Deeth, R. J.; Butler, J. S.; Habtemariam, A.; Newton, M. E.; Sadler, P. J. *Angew. Chem. Int. Ed.* **2013**, *52*, 4194-4197.
(12) Komatsu, H.; Shindo, Y.; Oka, K.; Hill, J. P.; Ariga, K. *Angew. Chem. Int. Ed.* **2014**, *53*, 3993-3995.
(13) Maenaka, Y.; Suenobu, T.; Fukuzumi, S. *J. Am. Chem. Soc.* **2012**, *134*, 9417-9427.
(14) Maenaka, Y.; Suenobu, T.; Fukuzumi, S. *J. Am. Chem. Soc.* **2012**, *134*, 367-374.
(15) Matsubara, C.; Kawamoto, N.; Takamura, K. *Analyst* **1992**, *117*, 1781-1784.
(16) Dickinson, B. C.; Huynh, C.; Chang, C. J. *J. Am. Chem. Soc.* **2010**, *132*, 5906–5915.
(17) Gay, C.; Collins, J.; Gebicki, J. M. *Anal. Biochem.* **1999**, *273*, 149-155.
(18) Baga, A. N.; Johnson, G. R. A.; Nazhat, N. B.; Saadalla-Nazhat, R. A. *Anal. Chim. Acta.* **1988**, *204*, 349-353.
(19) Onoda, M.; Uchiyama, T.; Mawatari, K.-i.; Kaneko, K.; Nakagomi, K. *Anal. Sci.* **2006**, *22*, 815-817.
(20) Shibata, S.; Suenobu, T.; Fukuzumi, S. *Angew. Chem. Int. Ed.* **2013**, *52*, 12327-12331.
(21) Hong, Y.; Sengupta, S.; Hur, W.; Sim, T. *J. Med. Chem.* **2015**, *58*, 3739-3750.
(22) Zhang, X.; Li, X.; Li, Z.; Wu, X.; Wu, Y.; You, Q.; Zhang, X. *Org. Lett.* **2018**, *20*, 3635-3638.
(23) Liu, Z.; Sadler, P. J. *Acc. Chem. Res.* **2014**, *47*, 1174-1185.



 

View Article Online
DOI: 10.1039/D0CC04970K

# COMMUNICATION



**Table of Content**

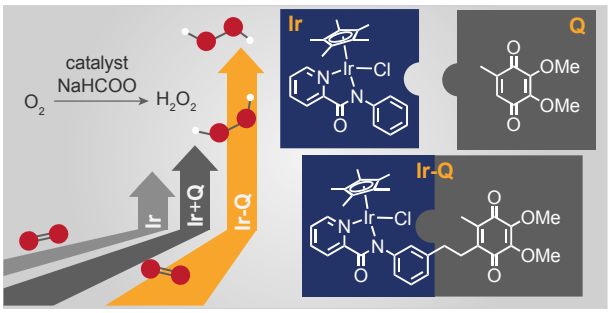


Tethered iridium-quinone catalyst in the presence of air and sodium formate generates $H_2O_2$ more rapidly than iridium and quinone mixtures at low catalyst concentration.